Contents lists available at ScienceDirect

Regenerative Therapy

Original Article

Biological function and application of melanocytes induced and transformed by mouse bone marrow mesenchymal stem cells

Yihui Xie [†], Ziqian Xu [†], Weimin Shi, Xingyu Mei[*]

Department of Dermatology, Shanghai General Hospital, Shanghai Jiao Tong University School of Medicine, Shanghai, China

ABSTRACT

Background: A large number of autologous melanocytes are required for surgical treatment of depigmentation diseases such as vitiligo. The purpose of this experiment is to explore the application of melanocytes induced by mesenchymal stem cells to clinical treatment. Therefore, we have induced mouse bone marrow mesenchymal stem cells (BMMSCs) into melanocytes (miMels) in the previous experiment. This experiment continues the previous experiment to further study the biological functions of miMels and their application in tissue engineering.
Methods: We examined whether miMels can produce active tyrosinase, melanin, and response to α-MSH. The ability of miMels to produce melanin to keratinocytes was tested by co-culture. By applying miMels to tissue-engineered skin, the survival and function of miMels on the surface of nude mice were verified.
Results: MiMels can produce active tyrosinase and melanin, and can pass melanin to the co-cultured keratinocytes. Under the stimulation of α-MSH, the active tyrosinase and melanin content of miMels increased. We tried to apply it to the establishment of tissue-engineered skin and obtained tissue-engineered skin containing miMels. Then we tried to transplant tissue-engineered skin on the back skin of nude mice and succeeded. The transplanted miMels survived in local tissues, synthesized active tyrosinase and melanin, and expressed the marker protein of melanocytes.
Conclusion: In short, miMels can be used as a cell source for tissue engineering skin. MiMels not only have a typical melanocyte morphology but also have the same biological functions as normal melanocytes. What's more important is its successful application in mouse tissue-engineered experiments.
© 2022, The Japanese Society for Regenerative Medicine. Production and hosting by Elsevier B.V. This is an open access article under the CC BY-NC-ND license (http://creativecommons.org/licenses/by-nc-nd/4.0/).

1. Introduction

Melanocytes that produce pigment are widely distributed throughout the body including the epidermis, hair follicles, and mucous membranes of some tissues [1,2]. The primary function of melanocytes originating from Nerve cells is the production of the melanin pigment [1,3]. Melanosomes require specific enzymes and structural proteins to be mature and become competent to produce melanin. Tyrosinase is a critical enzyme that catalyzes the rate-limiting steps of melanin biosynthesis [4].

Vitiligo is a multi-gene and multi-factor autoimmune disease which affects 0.3–0.5% of the population worldwide and the typical performance is the selective destruction of melanocytes [5]. The current treatment measures include local treatment, photo-therapies, surgical treatments, and others [6]. The surgical treatments conclude tissue grafts and cellular grafts which seem to have the same repair rates [7]. So far, there have been a series of successful cases of transplantation treatment. Vitiligo patients have been successfully treated with autologous non-cultured melanocyte-keratinocyte transplantation and cultured autologous pure melanocytes [8,9]. On account of the limited passage number of human melanocytes in vitro, a surgical treatment that relies on a large number of melanocytes has its limitations, which have to be settled urgently [10].

In recent years, translational and regenerative medicine shows that stem cells have important application value in melanocyte transformation mainly including human embryonic stem cells

---

(hESCs), pluripotent stem cells (iPSCs), and adult stem cells. The way to obtain hESCs is very limited and there are three key issues of hESCs that ethical issue, immunological issue, and safety issue [11,12]. Compared with hESCs, iPSCs successfully avoided immune rejection and ethical issues nevertheless some carcinogens and viral vectors are used in the process of inducing iPSCs, which affects the application safety [13]. As adult stem cells, Mesenchymal stem cells (MSCs) which play an important role in homeostasis and repair have the potential of multiple differentiation [14]. In addition, MSCs, because of the ability to regulate the host immune response thereby avoiding recipient recognition and subsequent rejection, become a valuable cell source for various cell transplantation therapies [15].

Some studies have shown the possibility and prospects of mesenchymal stem cells used in tissue engineering skin. The establishment of tissue-engineered skin must solve the problems of cells, scaffolds, and growth stimulation signals [16].MSCs have a variety of methods for tissue repair so they can be used for tissue-engineered skin [17]. MSCs derived from multiple sites (bone marrow, adipose tissue, amniotic fluid, and dermis) with multilineage differentiation, high frequency, ease of isolation and characterization, and the ability to migrate to injury are considered to be the main cell source [18]. The scaffold affects the adhesion and proliferation of KCs, fibroblasts, and MSCs [19]. Extracellular matrix (ECM) usually contains a variety of biologically active molecules, so it can provide support for surrounding cells and can affect cell adhesion, migration, differentiation, and the production of new ECM [20,21]. In addition, dermal cells, including fibroblasts and adipocytes, work with the scaffold to support epidermal function and integrity [22]. The collagen ECM of connective tissue can mimic the function of the target tissue, so it can be used as a scaffold for tissue-engineered skin [23].

There have been successful practices of inducing stem cells to melanocytes. T Yamane et al. derived melanocytes from cultured mouse embryonic stem cells [24]. Fang D et al. showed the differentiation process of human embryonic stem cells into melanocytes for the first time [25]. iPSC is used to generate embryonic bodies, which are then successfully differentiated into melanocytes by treatment with growth factors [26]. Hosaka C et al. successfully induced the melanocyte precursor cells derived from iPSC to differentiate into melanocytes [27]. Huang WS et al. transfected viral vectors into human adipose-derived stem cells to obtain iPSCs and then cultured them with an induction medium to obtain purified melanocytes [28]. Multilineage-differentiating stress enduring (Muse) cells, a new type of pluripotent stem cells derived from MSCs, have been isolated from human skin fibroblasts, human adipose stem cells, and bone marrow stem cells and can differentiate into functional melanocytes [29].

In 2015, we successfully induced mouse bone marrow mesenchymal stem cells (BMMSCs) into melanocytes (miMels). MiMels not only have a melanocyte-like morphology but also express specific markers and synthesize typical type III and type IV melanosomes in their cytoplasm [30]. This study will further explore whether miMels have the function of normal skin melanocytes, and try to apply them to tissue-engineered skin and carry out living transplantation. This experiment provides a meaningful exploration for the induction and transformation of human mesenchymal stem cells (hMSCs) into melanocytes for clinical treatment.

2. Methods

2.1. Cell source

In previous studies, we have successfully induced mouse BMMSCs to transform into melanocytes [30].

2.2. Determination of tyrosinase and melanin content

The cells were lysed and separated to obtain a supernatant containing active tyrosinase and a precipitate containing melanin. The protein in the supernatant was dissolved in PBS containing 0.1% L-DOPA, incubated at pH 6.8 and 37 °C for 30 min, and tyrosinase activity was measured at 475 nm using an ultraviolet spectrophotometer. The precipitate was dissolved in NaOH containing 10% DMSO at 80 °C for 1 h to obtain a solution containing melanin. The ultraviolet spectrophotometer measures the melanin content at 400 nm. Relative activity of tyrosinase = (A475 sample-blank group)/(A475 control-blank group); relative activity of melanin content = (A400 sample-blank group)/(A400 control-blank group).

2.3. Transwell co-culture

The 12W-induced miMels, B16 cells (positive control), and BMMSCs (negative control) were plated in the upper chamber of the Transwell Chamber, and co-cultured with the mouse keratinocytes (KCs) in the lower chamber of the Transwell Chamber for more than 7 days. Then the KCs in the lower chamber were stained with gp100 immunofluorescence to confirm whether the melanin synthesized and secreted by the upper chamber cells could be transported to the keratinocytes in the lower chamber to make it contain melanin.

2.4. RNA extraction

Take granulation tissue from the transplantation site, grind the tissue in liquid nitrogen, add TRIzol reagent (Invitrogen), and homogenize with a homogenizer. the sample volume should not exceed 10% of TRIzol. Take the clear homogenate, add 0.2 ml chloroform per 1 ml volume, shake vigorously for 15S, leave at room temperature for 5min, centrifuge at 10000g at 2–8 °C for 15min. Take the water phase, transfer to the ep tube, add an equal volume of isopropanol, leave it at room temperature for 10 min, centrifuge at 10000g at 2–8 °C for 10 min. Take the gelatinous white precipitate at the bottom of the tube, wash with 75% ice-cold ethanol, centrifuge and discard the supernatant.

2.5. Quantitative RT-PCR

Use reverse transcriptase M-MLV (Takara) and random primers to obtain cDNA from 1 μg of total RNA, with a final volume of 20 μL. SYBR Green (Takara) is used as a primer probe for Quantitative RT-PCR. The thermal cycling parameters used for qRT-RCR were: 95 °C for 2 min, 40 cycles of 95 °C for 15 s, 60 °C for 20 s, 72 °C for 20 s, and 39 cycles of 60–95 °C for 30 s. The relative transcription levels of TRP-1, TRP-2, MITF, and MART-1 were quantified by Applied Biosystem 7500 Real-Time PCR System.

Primer sequence: TRP-1, F: 5′-GAAAACGCACCTATTGGACATAAC-3′ and R: 5′-TAACAACGCAGCCACTACAGC-3'; TRP-2, F: 5′-CTTCCTAACCGCAGAGCAACT-3′ and R: 5′-CCCAGGATTCCAATGAC-CACT-3'; MITF, F: 5′-TCTGATCCCCAAGTCAAATGAT-3′ and R: 5′-TCTTCTGTCGGTTTTCAAGGTC-3'; MART-1, F:5′-ATGCCAAGAGAA-GATGCTCA-3′ and R: 5′- AGCATGTCTCAGGTGTCTCG -3'.

2.6. Western blot

The bicinchoninic acid assay (Pierce, Rockford, IL, USA) was used to determine the concentration of total protein extracted from the grafted granulation tissue. The protein samples were loaded on a 10% SDS-PAGE gel and separated by electrophoresis at 80 V for 45 min, and then at 120 V for about 1 h. Then transfer the separated protein to nitrocellulose membrane (Biotrace) by semi-dry blotting

at 25 V for 1 h. Block the blotting membrane, then put the blotting membrane and primary antibody at 4 °C Incubate overnight.

The primary antibodies consist of rat anti-mouse TRP-1 IgG (1:300; Abcam), rat anti-mouse Mitf IgG (1:600; Abcam), and rat anti-mouse TRP-2 IgG (1:800; Abcam)), rat anti-mouse MART-1 (1:1000; Abcam) and rabbit composition。 The incubated samples were washed 3 times with blocking buffer and then incubated with a secondary antibody consisting of FITC-labeled goat anti-rabbit IgG and CY3-labeled goat anti-rat IgG (1:5000; Chemicon) for 1 h. Wash the membranes 3 times with Tris buffered saline/Tween-20. Use ACT-U2/Image-proplus 5.0 (Nikon/Dell) to develop protein bands.

2.7. Immunofluorescence

Cut the granulation tissue at the transplantation site into slices and use gp100 fluorescent stain (1 : 50; Abcam) to label melanin. Place the slices in a solution containing gp100 at 37 °C 24 h a day. Then, the slides were washed 3 times with PBS, fixed with 4% formaldehyde for 20 min, and then washed 3 times with PBS. Use DAPI fluorescent stain (D9542, Sigma–Aldrich) to stain the nucleus. Use the ImageXpress Micro® Confocal High-Content Imaging System (Molecular Devices) to display the images.

2.8. Establishment of tissue-engineered skin

Dissolve rat tail collagen in acetic acid solution, take tail rat collagen solution, DMEM, and fetal bovine serum, and mix them evenly in a volume ratio of 8:1:1. Take 2 ml of the collagen gel into a 12-well plate and place it in a 37 °C incubator until the gel is completely solidified. Drop 1 ml of miMels containing 1×10^6 cells on the surface of collagen, add 3 ml culture medium and continue to culture for 3 days. Then add 1 ml of mouse KCs containing 1×10^6 cells, and continue to culture for 1 day. Then proceed to the air-liquid surface culture to the end of the culture on the 20th day. Take out the cultured tissue-engineered skin system, wrap it in paraffin paper, embed it in paraffin, dehydrate and section to form tissue-engineered skin.

2.9. Construction of an animal model of skin abrasion

The skin on the back of the nude mouse was disinfected and abraded with steel sand to form a round skin lesion about 1 cm in diameter. Collect induced melanocytes, and make a cell suspension inoculated on the ground wound, covered and fixed with sterile petrolatum gauze, and removed the gauze 2 weeks after transplantation.

2.10. HE staining

Fix the obtained granulation tissue with 10% formaldehyde and add alcohol to dehydrate after trimming and rinsing. Add xylene to the tissue and embed in wax. Cut the embedded wax block into slices. The slices are ironed, placed on a glass slide, and dried in a 45 °C thermostat. Use xylene to remove the paraffin from the section, stain with hematoxylin and eosin, add gum, and cover with a cover glass for sealing.

2.11. Silver staining

The sections made from granulation tissue were immersed in silver nitrate dye for staining, and the stained sections were observed under a microscope.

2.12. Statistical analysis

All data were expressed as mean ± SD. The student's t-test was used to calculate the statistical difference between the two groups. $P < 0.05$ was considered statistically significant.

3. Results

3.1. MiMels are capable of producing melanin and tyrosinase activity

Melanin is produced through a tyrosinase-dependent pathway, and the hydroxylation of tyrosine to dopaquinone is a key step [31]. Tyrosinase oxidizes tyrosine to dopaquinone, which then generates melanin precursors through non-enzymatic reactions [32]. Therefore, we take the active tyrosinase that can catalyze the oxidation reaction as the detection target, not the protein level of tyrosinase, which does not fully reflect the level of active tyrosinase that can catalyze the production of melanin. To explore whether miMels can produce active tyrosinase and melanin, we used an ultraviolet spectrophotometer to detect the tyrosinase activity and melanin content of miMels at different culture time points relative to uninduced cells. The results showed that the relative tyrosinase activity (Fig. 1a) and the relative melanin content (Fig. 1b) of miMels continued to increase with the extension of the culture time. After 6 weeks of cultivation, the relative tyrosinase activity and melanin content of miMels are significantly different ($p < 0.05$), respectively reaching 2.59 ± 0.78 and 2.28 ± 0.30. After 10 weeks of culture, the relative tyrosinase activity and melanin content of miMels further increased, reaching 5.59 ± 1.48 and 5.28 ± 0.42; after 15 weeks of cultivation, its relative tyrosinase activity and melanin content reached 10.17 ± 1.48 and 9.56 ± 0.98. The expression level of tyrosinase in melanoma is higher than that in normal melanocytes [33]. The miMels we induced are used as a normal cell source for surgical treatment of vitiligo, so the expression of tyrosinase is much lower than that of B16 cells, and the melanin produced by the reaction catalyzed by tyrosinase is relatively small.

3.2. α-MSH promotes the increase of tyrosinase activity of miMels and the synthesis of melanin

It is generally believed that active tyrosinase, rather than generalized tyrosinase protein, has the biological function of catalyzing the synthesis of melanin. Therefore, we use relative tyrosinase activity and melanin content as the detection target of miMels' response to α-MSH stimulation. 0.1uM α-MSH was added to miMels and B16 cells induced at 8, 10, 12, and 15 weeks, and tyrosinase activity and melanin content were detected after 24H and 48H, respectively. The results show that: miMels induced for 8 weeks and B16 cells have significant differences in the relative activity of tyrosinase before and after 24h stimulation with α-MSH ($p < 0.05$); miMels induced at 12 and 15 weeks and B16 cells have significant differences in the relative activity of tyrosinase before and after the 48H stimulation with α-MSH ($p < 0.05$) (Fig. 2a). MiMels induced 8, 10, 12, 15 weeks and B16 cells have significant differences in their relative melanin content before and after α-MSH stimulation for 24H and 48H ($p < 0.05$) (Fig. 2b). MC1R, the α-MSH receptor, is expressed in both melanocytes and melanoma cells, but the number of expressions in melanoma cells far exceeds that of normal melanocytes [34]. α-MSH binds to the receptor MC1R to generate a cascade reaction to activate tyrosinase [35]. b16 cell is a melanoma cell line. Compared with normal melanocytes, there are more MC1R receptors. The cascade reaction can greatly activate tyrosinase.
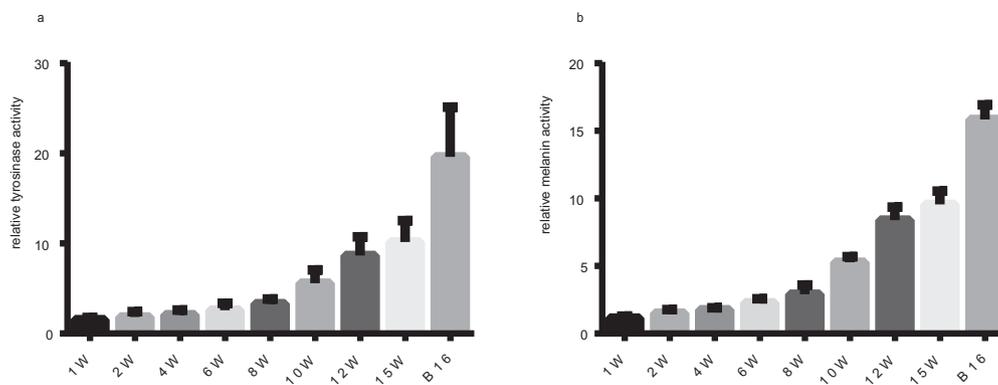
Fig. 1. The relative tyrosinase activity and melanin content of miMels. (a) UV spectrophotometer was used to detect the tyrosinase activity of miMels and B16 cells at different culture time points (1, 2, 4, 6, 8, 10, 12, 15 weeks) relative to uninduced cells. (b) UV spectrophotometer was used to detect the melanin content of miMels and B16 cells at different culture time points (1, 2, 4, 6, 8, 10, 12, 15 weeks) relative to uninduced cells.
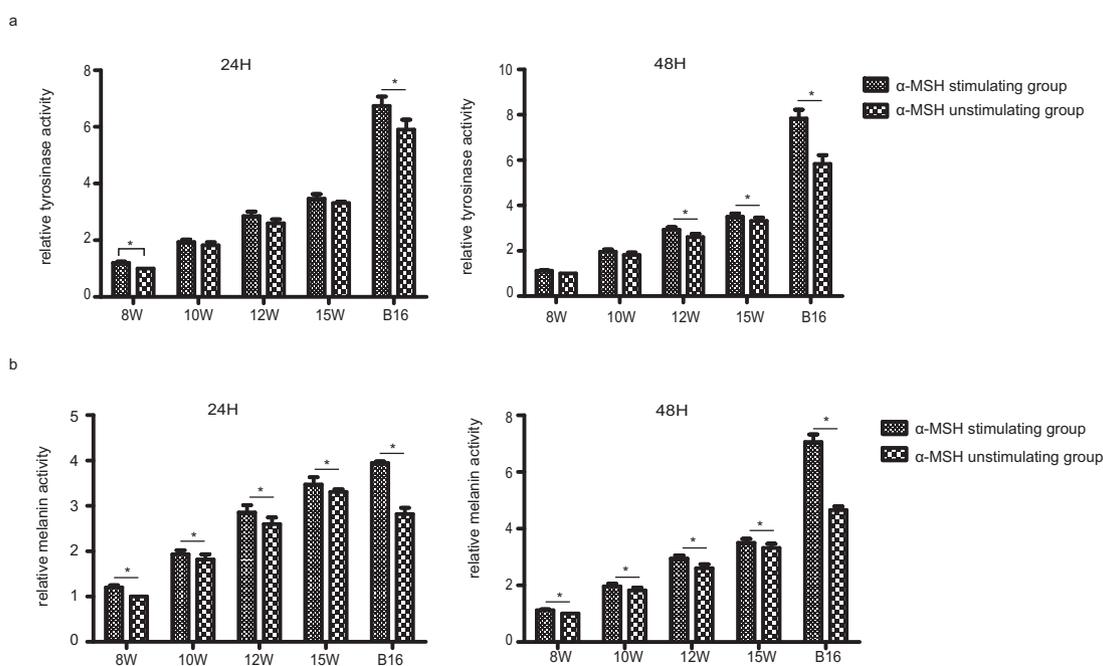

Fig. 2. The relative tyrosinase activity and melanin content of miMels induced at different time points stimulated with 0.1uMα-MSH at 24h and 48h. (a) 0.1uMα-MSH stimulated miMels induced at 8, 10, 12, and 15 weeks and B16 cells, and tyrosinase activity was detected by UV spectrophotometer at 24h and 48h, respectively. (b) 0.1uMα-MSH stimulated miMels induced at 8, 10, 12, and 15 weeks and B16 cells, and the relative melanin content of the cells was detected by an ultraviolet spectrophotometer at 24h and 48h, respectively.

Therefore, the response of miMels to α-MSH is weaker than that of b16 cells.

3.3. MiMels delivers the synthesized melanin to co-cultured KCs

Normal melanocytes pass mature melanosomes to KCs, and the main structural component of melanosomes is gp100 [36]. The expression of the corresponding protein of gp100 is limited to normal melanocytes and melanoma cells, which has strong specificity [37]. And in melanocytes, the formation of gp100 fibers is limited to melanosomes [38]. Therefore, we use gp100 as a specific marker of melanosomes to verify that miMels can deliver melanosomes to keratinocytes. In the epidermis, melanocytes transfer melanin pigment to KCs to achieve the photoprotective effect on the skin [39]. Therefore, whether melanin can be transferred to KCs is one of the keys to whether miMels can be used as normal epidermal melanocytes. B16 cells, mouse BMMSCs, and miMels induced for 12 weeks were respectively co-cultured with KCs, and then the KCs were stained by immunofluorescence. From the 11th day when miMels and KCs were co-cultured, the gp100 immunofluorescence staining of KCs was positive (Fig. 3). The above content shows that miMels induced for 12 weeks can deliver synthetic secreted melanin to co-cultured KCs.

3.4. Apply miMels to tissue engineering

To further explore the application of miMels in tissue engineering. We make miMels into tissue-engineered skin. The normal group represents normal skin, as a positive control; the material group represents tissue-engineered skin without miMels as a negative control; the experimental group is tissue-engineered skin
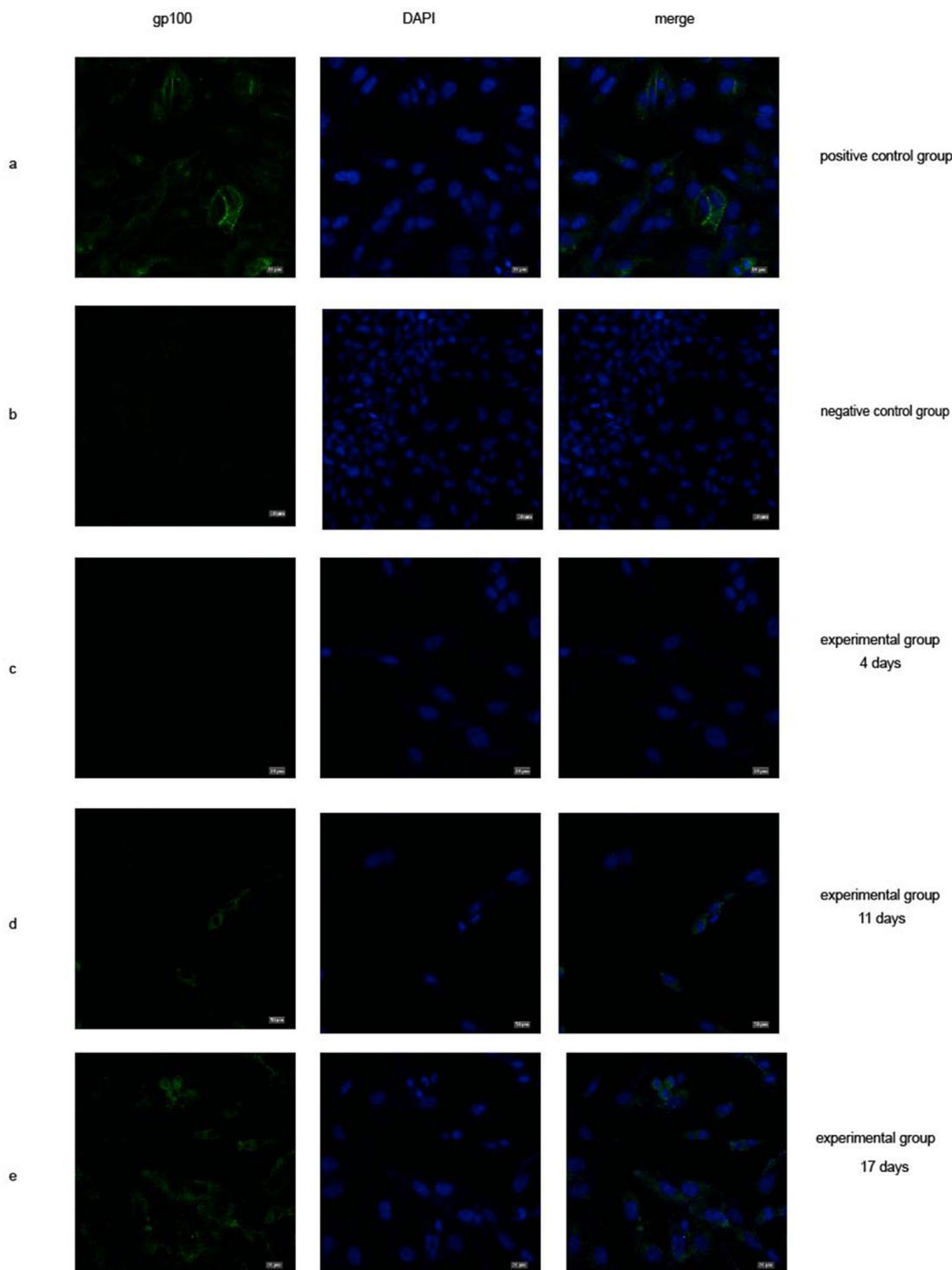
Fig. 3. The immunofluorescence staining of KCs co-cultured with the induced MSCs. (a) After 7 days of co-culture of B16 cells and KCs, gp100 immunofluorescence staining of KCs was positive. (b) After BMMSCs and KCs were co-cultured for 13 days, the gp100 immunofluorescence staining of KCs was negative. (c) After the BMMSCs induced for 12 weeks and KCs co-cultured for 4 days, the gp100 immunofluorescence staining of KCs was negative. (d) After the BMMSCs induced for 12 weeks and KCs co-cultured for 11days, the gp100 immunofluorescence staining of KCs showed a small amount of green fluorescence. (e) After the BMMSCs induced for 12weeks and KCs co-cultured for 17 days, the gp100 immunofluorescence staining of KCs was positive.

with miMels. HE staining is shown in Fig. 4a, it can be seen that compared with normal skin, tissue-engineered skin without miMels cannot form a clear skin structure; while tissue-engineered skin with miMels has a structure similar to the epidermis and dermis: the epidermis has multiple layers of KCs, and miMels are

evenly distributed among the KCs, the dermis is an irregular loose network structure without obvious stratification, and it intersects with the epidermis. The silver plating dyeing is shown in Fig. 4b, in normal skin, melanin particles were scattered in epidermal cells, no melanin particles were stained in the material group, and melanin
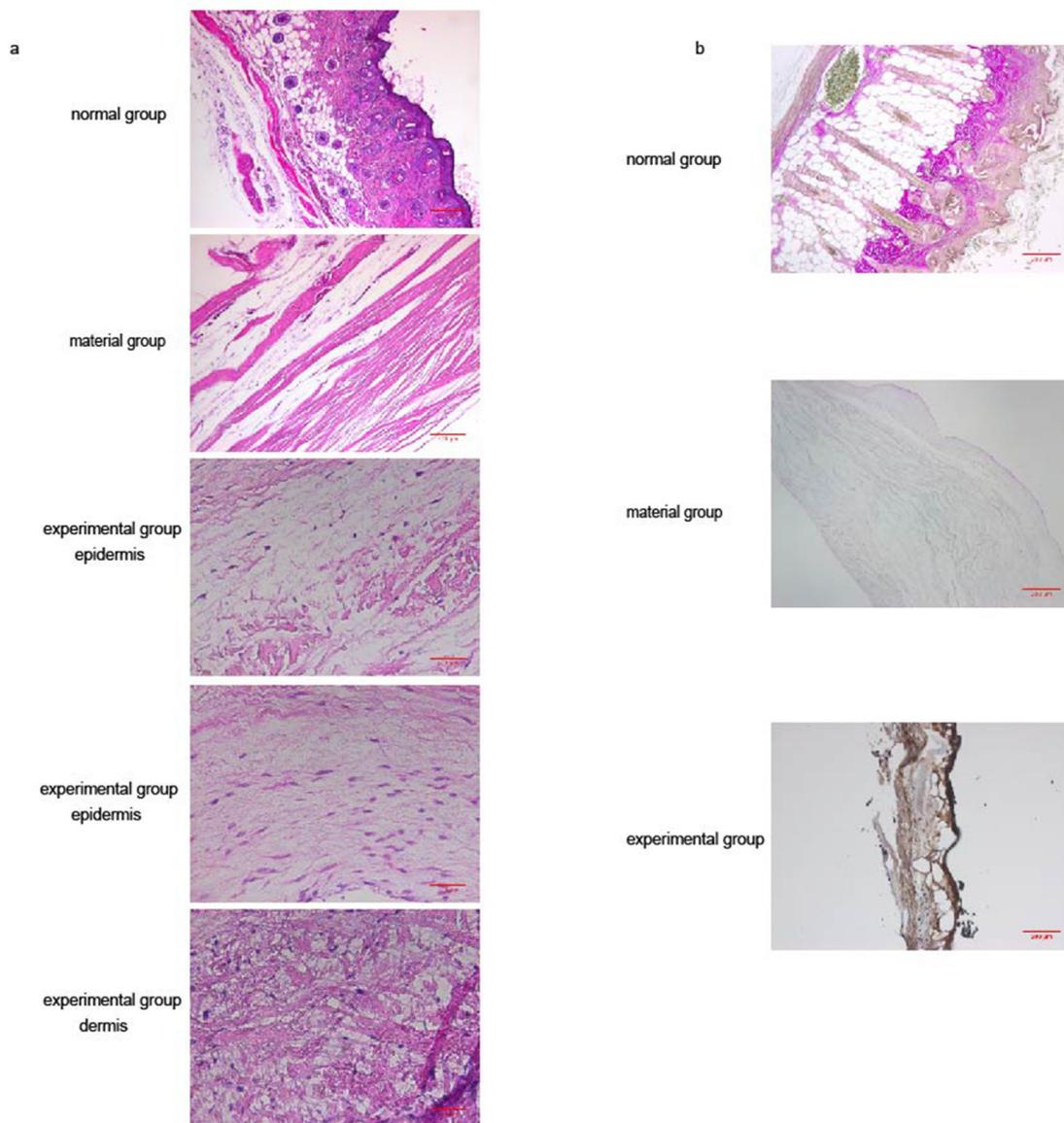
Fig. 4. The HE staining and the silver staining of miMels tissue-engineered skin. (a) HE staining results of normal group (normal skin), material group (tissue-engineered skin without miMels) and experimental group (tissue-engineered skin with miMels). (b) Silver staining results of normal group (normal skin), material group (tissue-engineered skin without miMels) and experimental group (tissue-engineered skin with miMels).

particles in the experimental group were distributed in all layers of the skin. Tissue-engineered skin lacks the role of a basement membrane band compared with normal skin, the proliferation and migration of miMels were not limited, so the dermis also has scattered miMels distribution. This problem needs to be solved urgently.

3.5. The miMels tissue-engineered skin was tentatively applied to the skin of nude mice

Cell suspensions were prepared and divided into the model group (PBS), BMMSCs group (BMMSCs count 1×10^6), low-dose group (miMels count 1×10^5), medium-dose group (miMels count 5×10^5) and high-dose group (miMels count 1×10^6). About 1 ml volume of miMels cell suspension was inoculated on the ground wound on the back of nude mice. Two weeks later, the granulation tissue from the transplantation site was taken. After 2

weeks, the macroscopic view of the mice (Fig. 5a), HE staining of granulation tissue (Fig. 5a) and gp100 fluorescent staining (Fig. 5b) are shown in the figure. In the macroscopic view, from left to right are the model groups, low-dose group (miMels count 1×10^5), medium-dose group (miMels count 5×10^5) and high-dose group (miMels count 1×10^6). Since the initial grinding area is the same, it is obvious that with the increase of miMels, the growth trend of the mouse skin is better. In the HE stained pictures, the normal group represents normal skin. It can be seen that with the increase in the number of implanted miMels, the granulation tissue appeared closer to normal skin, especially in the high-dose group; however, in the model group and BMMSCs group, the morphology of the granulation tissue was far from normal skin. The gp100 fluorescent staining showed that as the number of transplanted miMels cells increased, the melanin particles in the tissues also increased, and the model group and BMMSCs group could not produce the same results as the miMel (Fig. 5b). Western-blot
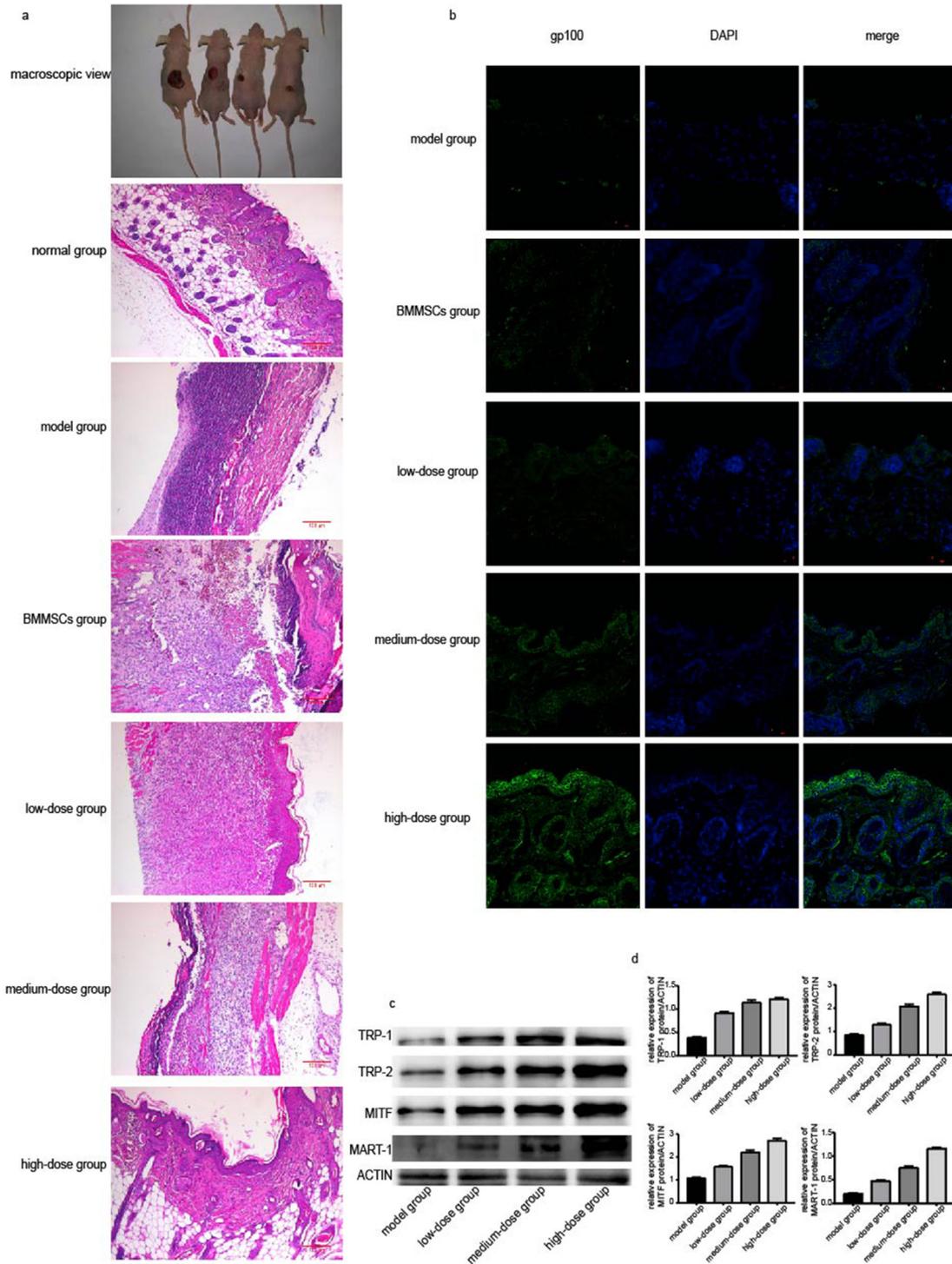
Fig. 5. The structure and the relevant protein expression of the transplanted tissue. (a) Macroscopic view of mice cultured for 2 weeks, from left to right represent the model group (PBS), low-dose group (miMels count 1×10^5), medium-dose group (miMels count 5×10^5), and high-dose group (miMels count 1×10^6), respectively. HE stained pictures of normal group (normal skin), model group (PBS), BMMSCs group (BMMSCs count 1×10^6), low-dose group (miMels count 1×10^5), medium-dose group (miMels count 5×10^5), and high-dose group (miMels count 1×10^6) transplanted tissue. (b) The gp100 immunofluorescence staining of the model group (PBS), BMMSCs group (BMMSCs count 1×10^6), low-dose group (miMels count 1×10^5), medium-dose group (miMels count 5×10^5), high-dose group (miMels count 1×10^6) transplanted tissues shows the distribution of melanin particles in the epidermis and dermis. (c) The expression of TRP-1, TRP-2, MITF, and MART-1 in the transplanted tissues of the model, low-dose, medium-dose, and high-dose groups were determined by Western blot. (d) The gray value statistics of the protein expression levels of TRP-1, TRP-2, MITF, and MART-1 in the transplanted tissues in the model, low-dose, medium-dose, and high-dose group was determined.

(Fig. 5c—d) showed that the expressions of TRP-1, TRP-2, MITF, and MART-1 in the miMels cell transplantation group were higher than those in the model group, and as the number of miMels increased, the expression of related proteins also increased.

4. Discussion

In the previous study, we successfully induced the transformation of mouse BMMSCs into miMels. And through optimization, the conversion time was shortened from 120 days to 90 days, and the passage cycle was also shortened from 14-16 days to 4—5 days [30]. L-DOPA staining and UV spectrophotometric detection of miMels confirmed that: The miMels obtained by the induced transformation have the morphology of typical melanocytes, active tyrosinase, and can synthesize melanin. With the extension of the induction time, the tyrosinase activity of the transformed cells increased, the synthesis of melanin increased, and they responded to α-MSH stimulation. α-MSH is the main product of Proopiomelanocortin in the skin, which increases the synthesis of melanin and changes the morphology of melanocytes [40]. It also regulates skin immunity, protects the skin from immune system damage, UVR-induced apoptosis, and DNA damage, and interacts with pathogens effects [41]. In the co-culture of miMels and KCs, the Transwell co-culture experiment proved that miMels can deliver the melanin synthesized and secreted to the co-cultured KCs. These experimental results indicate that miMels have the biological activities and functions of normal melanocytes. We tried to make miMels, KCs and rat tail collagen into tissues similar to tissue-engineered skin, with a structure similar to the epidermis and dermis. The silver staining of the tissue sections showed that the epidermal cells were interspersed with melanin particles, which indicated that miMels could be used in tissue-engineered skin and survive and synthesize melanin particles. We inoculated miMels on the back of nude mice. The new granulation tissue at the transplantation site had a normal epidermal dermal structure. As the number of transplanted miMels increased, the melanin particles in the tissue increased, and the expression of the related proteins (TRP-1, TRP-2, MITF, and MART- 1) also increased. It can be seen that miMels can survive in local tissues after being transplanted into living skin, synthesize and secrete melanin particles to the epidermis and dermis, and express the marker proteins of normal melanocytes. We successfully transformed BMMSCs into melanocytes, and then combined with tissue engineering and conducted animal experiments. This is a huge advancement in mesenchymal stem cells from induced transformation to application. The research on cells is no longer limited to the cells themselves, but extends to tissue-engineered skin with therapeutic value, which has practical and exploratory significance.

At present, the experimental methods used by miMels for tissue-engineered skin preparation cannot obtain tissue sections with typical epidermal and dermal structures. Therefore, in future experiments, it is necessary to try to use more tissue engineering materials and explore more effective tissue engineering skin slice preparation methods. Our research confirmed the feasibility of miMels applied to tissue-engineered skin and autologous cell transplantation treatment. The above attempts on mouse mesenchymal stem cells provide a theoretical and experimental basis for further inducing human mesenchymal stem cells to transform into active melanocytes in vitro and for their use in vitiligo tissue engineering and translational medicine treatment. However, the source selection of human mesenchymal stem cells, the method of inducing transformation, the expansion of melanocytes after transformation, and the biological activity, immunogenicity, and biological safety of transformed cells all need to continue to be explored.

5. Conclusion

In short, miMels can be used as a cell source for tissue engineering skin. MiMels not only have a typical melanocyte morphology but also has the same biological functions as normal melanocytes. What's more important is its successful application in mouse tissue engineered experiment.

Data availability

Not applicable.

Ethics approval

The animal experiment described in this article was approved by the Animal Ethics Committee of Shanghai First People's Hospital.

Authors' contributions

Conceptualization, Yihui Xie and Xingyu Mei; Data curation, Yihui Xie; Formal analysis, Yihui Xie; Funding acquisition, Yihui Xie; Investigation, Yihui Xie; Methodology, Yihui Xie; Project administration, Yihui Xie; Resources, Yihui Xie; Software, Yihui Xie; Supervision, Yihui Xie; Validation, Yihui Xie; Visualization, Yihui Xie; Writing − original draft, Yihui Xie and Ziqian Xu; Writing − review & editing, Yihui Xie, Weimin Shi and Xingyu Mei.

Declaration of competing interest

None.

Acknowledgements

References

[1] Bandarchi B, Jabbari CA, Vedadi A, Navab R. Molecular biology of normal melanocytes and melanoma cells. J Clin Pathol 2013;66(8):644—8.

[2] Yamaguchi Y, Hearing VJ. Melanocytes and their diseases. Cold Spring Harb Perspect Med 2014;4(5).

[3] D'Mello SA, Finlay GJ, Baguley BC, Askarian-Amiri ME. Signaling pathways in melanogenesis. Int J Mol Sci 2016;17(7).

[4] Spritz RA. Molecular genetics of oculocutaneous albinism. Hum Mol Genet 1994;3 Spec:1469—75.

[5] Birlea SA, Costin GE, Roop DR, Norris DA. Trends in regenerative medicine: repigmentation in vitiligo through melanocyte stem cell mobilization. Med Res Rev 2017;37(4):907—35.

[6] Ezzedine K, Eleftheriadou V, Whitton M, van Geel N. Vitiligo. Lancet 2015;386(9988):74—84.

[7] Gawkrodger DJ, Ormerod AD, Shaw L, Mauri-Sole I, Whitton ME, Watts MJ, et al. Guideline for the diagnosis and management of vitiligo. Br J Dermatol 2008;159(5):1051—76.

[8] Altalhab S, AlJasser MI, Mulekar SV, Al Issa A, Mulekar S, Diaz J, et al. Six-year follow-up of vitiligo patients successfully treated with autologous non-cultured melanocyte-keratinocyte transplantation. J Eur Acad Dermatol Venereol 2019;33(6):1172—6.

[9] Chen YF, Yang PY, Hu DN, Kuo FS, Hung CS, Hung CM. Treatment of vitiligo by transplantation of cultured pure melanocyte suspension: analysis of 120 cases. J Am Acad Dermatol 2004;51(1):68—74.

[10] Nielsen HI, Don P. Culture of normal adult human melanocytes. Br J Dermatol 1984;110(5):569—80.

[11] Volarevic V, Markovic BS, Gazdic M, Volarevic A, Jovicic N, Arsenijevic N, et al. Ethical and safety issues of stem cell-based therapy. Int J Med Sci 2018;15(1):36—45.

[12] Barrilleaux B, Knoepfler PS. Inducing iPSCs to escape the dish. Cell Stem Cell 2011;9(2):103—11.

[13] Hockemeyer D, Soldner F, Cook EG, Gao Q, Mitalipova M, Jaenisch R. A drug-inducible system for direct reprogramming of human somatic cells to pluripotency. Cell Stem Cell 2008;3(3):346–53.

[14] Hwang NS, Zhang C, Hwang YS, Varghese S. Mesenchymal stem cell differentiation and roles in regenerative medicine. Wiley Interdiscip Rev Syst Biol Med 2009;1(1):97–106.

[15] Uccelli A, Moretta L, Pistoia V. Immunoregulatory function of mesenchymal stem cells. Eur J Immunol 2006;36(10):2566–73.

[16] Chan BP, Leong KW. Scaffolding in tissue engineering: general approaches and tissue-specific considerations. Eur Spine J 2008;17(Suppl 4):467–79. Suppl 4.

[17] Sun K, Zhou Z, Ju X, Zhou Y, Lan J, Chen D, et al. Combined transplantation of mesenchymal stem cells and endothelial progenitor cells for tissue engineering: a systematic review and meta-analysis. Stem Cell Res Ther 2016;7(1):151.

[18] Nourian Dehkordi A, Mirahmadi Babaheydari F, Chehelgerdi M, Raeisi Dehkordi S. Skin tissue engineering: wound healing based on stem-cell-based therapeutic strategies. Stem Cell Res Ther 2019;10(1):111.

[19] Bhowmick S, Rother S, Zimmermann H, Lee PS, Moeller S, Schnabelrauch M, et al. Biomimetic electrospun scaffolds from main extracellular matrix components for skin tissue engineering application - the role of chondroitin sulfate and sulfated hyaluronan. Mater Sci Eng C Mater Biol Appl 2017;79:15–22.

[20] Yi S, Ding F, Gong L, Gu X. Extracellular matrix scaffolds for tissue engineering and regenerative medicine. Curr Stem Cell Res Ther 2017;12(3):233–46.

[21] Varkey M, Ding J, Tredget EE. The effect of keratinocytes on the biomechanical characteristics and pore microstructure of tissue engineered skin using deep dermal fibroblasts. Biomaterials 2014;35(36):9591–8.

[22] Shook BA, Wasko RR, Rivera-Gonzalez GC, Salazar-Gatzimas E, López-Giráldez F, Dash BC, et al. Myofibroblast proliferation and heterogeneity are supported by macrophages during skin repair. Science 2018;362(6417).

[23] Goh KL, Holmes DF. Collagenous extracellular matrix biomaterials for tissue engineering: lessons from the common sea urchin tissue. Int J Mol Sci 2017;18(5).

[24] Yamane T, Hayashi S, Mizoguchi M, Yamazaki H, Kunisada T. Derivation of melanocytes from embryonic stem cells in culture. Dev Dynam 1999;216(4–5):450–8.

[25] Fang D, Leishear K, Nguyen TK, Finko R, Cai K, Fukunaga M, et al. Defining the conditions for the generation of melanocytes from human embryonic stem cells. Stem Cell 2006;24(7):1668–77.

[26] Yang R, Jiang M, Kumar SM, Xu T, Wang F, Xiang L, et al. Generation of melanocytes from induced pluripotent stem cells. J Invest Dermatol 2011;131(12):2458–66.

[27] Hosaka C, Kunisada M, Koyanagi-Aoi M, Masaki T, Takemori C, Taniguchi-Ikeda M, et al. Induced pluripotent stem cell-derived melanocyte precursor cells undergoing differentiation into melanocytes. Pigment Cell Melanoma Res 2019;32(5):623–33.

[28] Huang WS, Wei LG, Li JK, Fu KY, Huang TC, Hsieh PS, et al. Melanocyte differentiation from induced pluripotent stem cells derived from human adipose-derived stem cells. Ann Plast Surg 2019;82(1S Suppl 1). S119-s25.

[29] Yamauchi T, Yamasaki K, Tsuchiyama K, Koike S, Aiba S. The potential of muse cells for regenerative medicine of skin: procedures to reconstitute skin with muse cell-derived keratinocytes, fibroblasts, and melanocytes. J Invest Dermatol 2017;137(12):2639–42.

[30] Mei X, Sun Y, Wu Z, Pan W, Zhu J, Shi W. In vitro-induced differentiation of bone marrow mesenchymal stem cells into melanocytes. Cell Biol Int 2015;39(7):824–33.

[31] Lin JY, Fisher DE. Melanocyte biology and skin pigmentation. Nature 2007;445(7130):843–50.

[32] Land EJ, Ramsden CA, Riley PA. Tyrosinase autoactivation and the chemistry of ortho-quinone amines. Acc Chem Res 2003;36(5):300–8.

[33] Hill R, Kalathur RK, Colaço L, Brandão R, Ugurel S, Futschik M, et al. TRIB2 as a biomarker for diagnosis and progression of melanoma. Carcinogenesis 2015;36(4):469–77.

[34] Cummins DL, Cummins JM, Pantle H, Silverman MA, Leonard AL, Chanmugam A. Cutaneous malignant melanoma. Mayo Clin Proc 2006;81(4):500–7.

[35] Rosenkranz AA, Slastnikova TA, Durymanov MO, Sobolev AS. Malignant melanoma and melanocortin 1 receptor. Biochemistry (Mosc) 2013;78(11):1228–37.

[36] Yamaguchi Y, Hearing VJ. Physiological factors that regulate skin pigmentation. Biofactors 2009;35(2):193–9.

[37] Slominski A. Coming of age of melanogenesis-related proteins. Arch Pathol Lab Med 2002;126(7):775–7.

[38] Bissig C, Rochin L, van Niel G. PMEL amyloid fibril formation: the bright steps of pigmentation. Int J Mol Sci 2016;17(9).

[39] Domingues L, Hurbain I, Gilles-Marsens F, Sirés-Campos J, André N, Dewulf M, et al. Coupling of melanocyte signaling and mechanics by caveolae is required for human skin pigmentation. Nat Commun 2020;11(1):2988.

[40] Millington GW. Proopiomelanocortin (POMC): the cutaneous roles of its melanocortin products and receptors. Clin Exp Dermatol 2006;31(3):407–12.

[41] Donnarumma G, Paoletti I, Buommino E, Tufano MA, Baroni A. Alpha-MSH reduces the internalization of Staphylococcus aureus and down-regulates HSP 70, integrins and cytokine expression in human keratinocyte cell lines. Exp Dermatol 2004;13(12):748–54.